

The effect of Ti addition on alloying and formation of nanocrystalline structure in Fe–Al system

M. Rafiei · M. H. Enayati · F. Karimzadeh

Received: 22 November 2009 / Accepted: 6 April 2010 / Published online: 22 April 2010
© Springer Science+Business Media, LLC 2010

Abstract In this work, the effect of Ti addition on alloying and formation of nanocrystalline structure in Fe–Al system was studied by utilizing mechanical alloying (MA) process. Structural and morphological evolutions of powder particles were studied by X-ray diffractometry, microhardness measurements, and scanning electron microscopy. In both $\text{Fe}_{75}\text{Al}_{25}$ and $\text{Fe}_{50}\text{Al}_{25}\text{Ti}_{25}$ systems MA led to the formation of Fe-based solid solution which transformed to the corresponding intermetallic compounds after longer milling times. The results indicated that the Ti addition in Fe–Al system affects the phase transition during mechanical alloying, the final crystallite size, the mean powder particle size, the hardness value and ordering of DO_3 structure after annealing. The crystallite size of Fe_3Al and $(\text{Fe},\text{Ti})_3\text{Al}$ phases after 100 h of milling time were 35 and 12 nm, respectively. The Fe_3Al intermetallic compound exhibited the hardness value of 700 Hv which is significantly smaller than 1050 Hv obtained for $(\text{Fe},\text{Ti})_3\text{Al}$ intermetallic compound.

Introduction

Intermetallic phases have attracted significant interests during the last few decades since they offer new prospects for developing structural materials for high temperature applications [1].

Iron aluminides based on Fe_3Al intermetallic are currently receiving extensive study as they include several advantages over other iron base alloys such as lower

density, high specific strengths, and good oxidation and corrosion resistance [2–4].

The alloys based on Fe_3Al are generally stronger than those based on FeAl , at least at temperatures where they maintain the DO_3 ordered state, and thus have interest for certain applications even though their density advantage and oxidation resistance may not be as good as that of the FeAl materials [5]. Commercialization of these intermetallics has been very limited due to the low ductility and impact resistance at ambient temperature as well as poor creep strength at elevated temperatures [6]. In order to overcome these problems, there are two main approaches: (1) alloying of this compounds with third element such as Ti, Cr ... and (2) control of crystallite size and its morphology [7]. There are several ways of intermetallic compounds synthesis including mechanical alloying (MA). This method additionally is capable of producing nanocrystalline structure [8].

Maupin et al. [9] reported that addition of Ti to Fe_3Al can improve its tribological properties. This suggests that iron aluminides may find their applications in some tribological circumstances, especially where the oxidation or sulfidation is also a major concern. Zhu et al. [6] investigated the effect of Ti on the microstructure and mechanical properties of Fe_3Al prepared by arc-melting method and reported that the addition of Ti is effective in refining the coarse grained microstructures of Fe_3Al and significantly improves the high strength to higher temperatures. Zhu and Iwasaki [10] studied MA of Fe–Al–Ti system with different molar ratio of Ti. They found that addition of Ti to Fe–Al binary system reduces the particle size and crystallite size of final product and increases the kinetics of solid solution formation. This work was aimed to synthesize Fe_3Al intermetallic compound and to study the effect of Ti on alloying and nanocrystallization processes during

M. Rafiei · M. H. Enayati (✉) · F. Karimzadeh
Department of Materials Engineering, Isfahan University
of Technology, 84156-83111 Isfahan, Iran
e-mail: ena78@cc.iut.ac.ir

mechanical alloying in comparison to those reported in our previous work [11].

Experimental methods

Fe (99.8% purity, $\sim 100 \mu\text{m}$) and Al (99.5% purity, ~ 50 – $100 \mu\text{m}$) elemental powders were used as original materials. In order to produce Fe_3Al compound, the powders were mixed with the nominal composition of $\text{Fe}_{75}\text{Al}_{25}$.

MA was carried out in a high energy planetary ball mill under argon atmosphere and at room temperature. The milling media consisted of five 20 mm diameter balls confined in a 120 mL volume vial. The ball and vial materials were hardened chromium steel. Ball to powder weight ratio and rotation speed of vial were 10:1 and 500 rpm, respectively. The total powder mass was 17 g. No process control agent (PCA) was added to powder mixture. Samples were withdrawn after selected time intervals and characterized by X-ray diffraction (XRD) in a Philips X'PERT MPD diffractometer using filtered $\text{Cu K}\alpha$ radiation ($\lambda = 0.1542 \text{ nm}$). Morphology of powder particles was characterized by scanning electron microscopy (SEM) in a Philips XL30. The mean powder particle size was estimated from SEM images of powder particles by image tool software. The average size of about 50 particles was calculated and reported as mean powder particle size. Isothermal annealing was carried out to study the thermal behavior of milled powders. MA samples were sealed and then annealed in a conventional furnace. The structural transitions occurred during annealing were determined by XRD. The hardness of cross-section of powder particles was also determined by microhardness test using a Vickers indenter at the load of 100 g and dwell time of 5 s. The average of five measurements for each sample was calculated and reported as hardness value.

Results and discussion

Figure 1 shows XRD patterns of $\text{Fe}_{75}\text{Al}_{25}$ powder mixture at different milling times. For as-received powders only Fe and Al diffraction peaks can be seen. There is no significant change in Fe and Al diffraction peaks with increasing milling time up to 40 h except weakening and broadening of these peaks due to the gradual refinement of crystallite size and enhancement of internal strain induced by increasing number of lattice defects during MA.

After 60 h of milling time, a $\text{Fe}(\text{Al})$ solid solution was formed as a result of diffusion of Al atoms in Fe lattice. The lattice parameter of $\text{Fe}(\text{Al})$ solid solution was calculated to be about 2.8 Å. This is accompanied by a shift in diffraction peaks of Fe toward lower angles as indicated in Fig. 2.

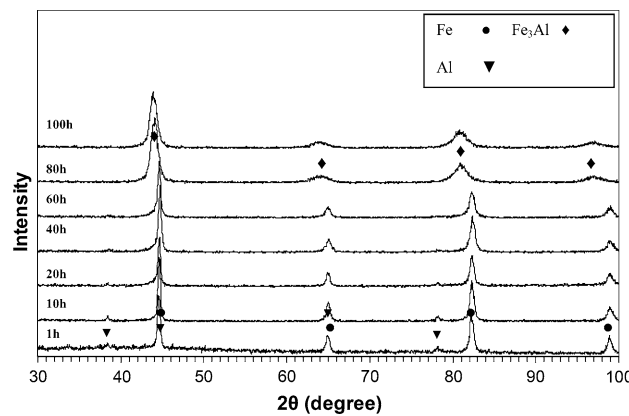


Fig. 1 XRD patterns of $\text{Fe}_{75}\text{Al}_{25}$ powder mixture at different milling times

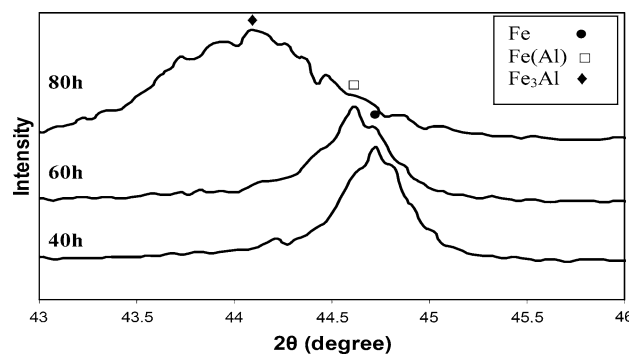


Fig. 2 Displacement of Fe (110) diffraction peak toward lower angles

Further milling led to the formation of Fe_3Al intermetallic compound which is accompanied by a further displacement of XRD peaks (Figs. 1, 2). The lattice parameter of this phase was calculated to be about 5.8 Å. The lack of superlattice diffraction peaks for Fe_3Al phase on XRD patterns indicates this phase has a disordered DO_3 structure. XRD results suggest that Fe_3Al compound was completely formed after 80 h MA. Increasing milling time up to 100 h did not change the phase composition significantly.

XRD patterns of $\text{Fe}_{50}\text{Al}_{25}\text{Ti}_{25}$ powder mixture are shown in Fig. 3. Similar to $\text{Fe}_{75}\text{Al}_{25}$ composition the intensity of crystalline diffraction peaks decreases and their width increases progressively with increasing milling time. Moreover, Fe (110) peak shifts toward lower angles (Fig. 4) after 10 h MA indicating that Al and Ti atoms dissolve in Fe lattice during milling and therefore a $\text{Fe}(\text{Al},\text{Ti})$ solid solution with bcc structure is formed. Further milling led to the formation of $(\text{Fe},\text{Ti})_3\text{Al}$ intermetallic compound after 40 h of milling time with disordered DO_3 structure before the complete solution of Al and Ti.

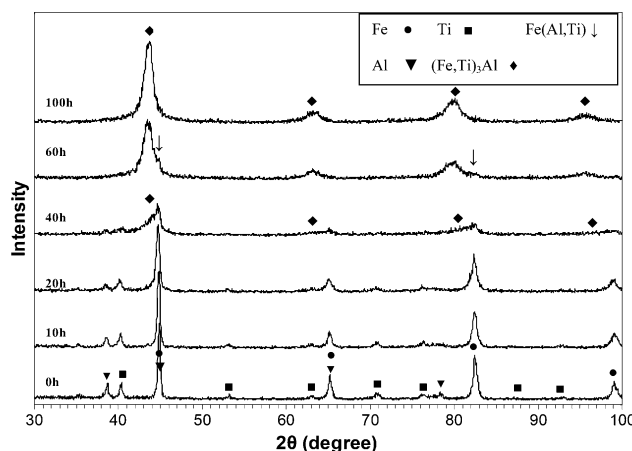


Fig. 3 XRD patterns of $\text{Fe}_{50}\text{Al}_{25}\text{Ti}_{25}$ powder mixture at different milling times [11]

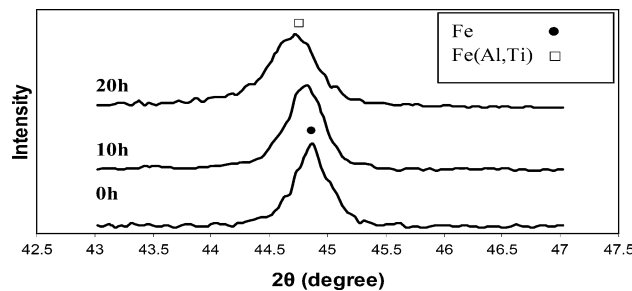


Fig. 4 Displacement of Fe (110) diffraction peak toward lower angles

Comparison of XRD patterns for Fe-Al and Fe-Al-Ti systems shows that in Fe-Al system the Fe-based solid solution starts to form at longer milling times compared with Fe-Al-Ti system. Also Fe_3Al intermetallic compound was formed between 60 and 80 h of milling times while $(\text{Fe},\text{Ti})_3\text{Al}$ intermetallic compound was obtained after 40 h indicating that Ti substitution for Fe in Fe_3Al phase decreases the milling time for intermetallic compound formation.

Figures 5 and 6 show XRD patterns from Fe_3Al and $(\text{Fe},\text{Ti})_3\text{Al}$ powder mixtures as-milled for 100 h and after subsequent annealing at 550 °C for 1 h. As seen in Fig. 5 after annealing no new phase was formed. The lack of superlattice diffraction peaks in annealed sample indicates that the disordered structure of the as-milled Fe_3Al remained unchanged after this heat treatment. Same behavior was previously reported by Enayati and Salehi [12] for Fe_3Al compound prepared by MA. Similar to $\text{Fe}_{75}\text{Al}_{25}$ powder mixture, no new phase formed after annealing of as-milled $\text{Fe}_{50}\text{Al}_{25}\text{Ti}_{25}$ powder mixture (Fig. 6), but in contrast to $\text{Fe}_{75}\text{Al}_{25}$, the superlattice diffraction peaks were observed. This indicates that Ti substitution for Fe in Fe_3Al phase increases the ordering of DO_3 structure upon annealing. Zhu and Iwasaki [10] also

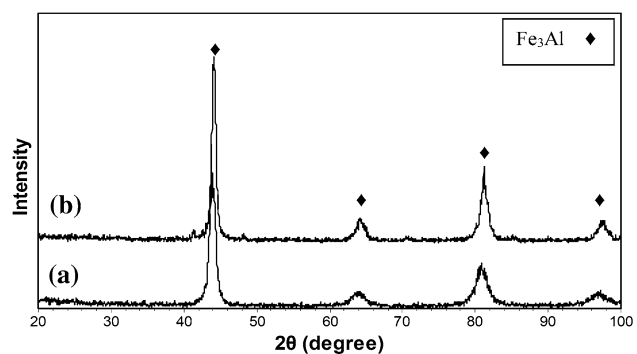


Fig. 5 XRD patterns of $\text{Fe}_{75}\text{Al}_{25}$ powder mixture (a) after 100 h MA and (b) after annealing at 550 °C for 1 h

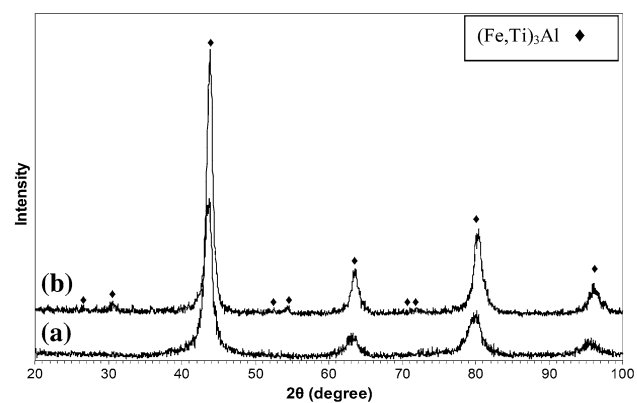


Fig. 6 XRD patterns of $\text{Fe}_{50}\text{Al}_{25}\text{Ti}_{25}$ powder mixture (a) after 100 h MA and (b) after annealing at 550 °C for 1 h [11]

reported that Ti substitution for Fe in Fe_3Al compound increases the ordering of DO_3 structure after annealing.

Crystallite size and internal strain of Fe_3Al and $(\text{Fe},\text{Ti})_3\text{Al}$ phases before and after annealing are presented in Table 1. The crystallite size and internal strain were calculated by analyzing XRD peaks broadening using the Williamson and Hall method [13]. The crystallite size of $(\text{Fe},\text{Ti})_3\text{Al}$ after 100 h of milling time was 12 nm which is smaller than 35 nm obtained for Fe_3Al phase. This suggests that the presence of Ti in Fe_3Al lattice increases the work hardening rate leading to predomination of dislocations production over recovery phenomena and therefore reducing the crystallite size.

For both $(\text{Fe},\text{Ti})_3\text{Al}$ and Fe_3Al phases annealing had more significant effect on reducing internal strain than for increasing of crystallite size. It is worth noting the crystallite size before and after annealing is the same within the experimental errors.

SEM images of powder particles for $\text{Fe}_{75}\text{Al}_{25}$ and $\text{Fe}_{50}\text{Al}_{25}\text{Ti}_{25}$ powder mixture at different milling times are shown in Figs. 7 and 8. As seen in Fig. 7 for $\text{Fe}_{75}\text{Al}_{25}$ system the mean powder particle size decreased with

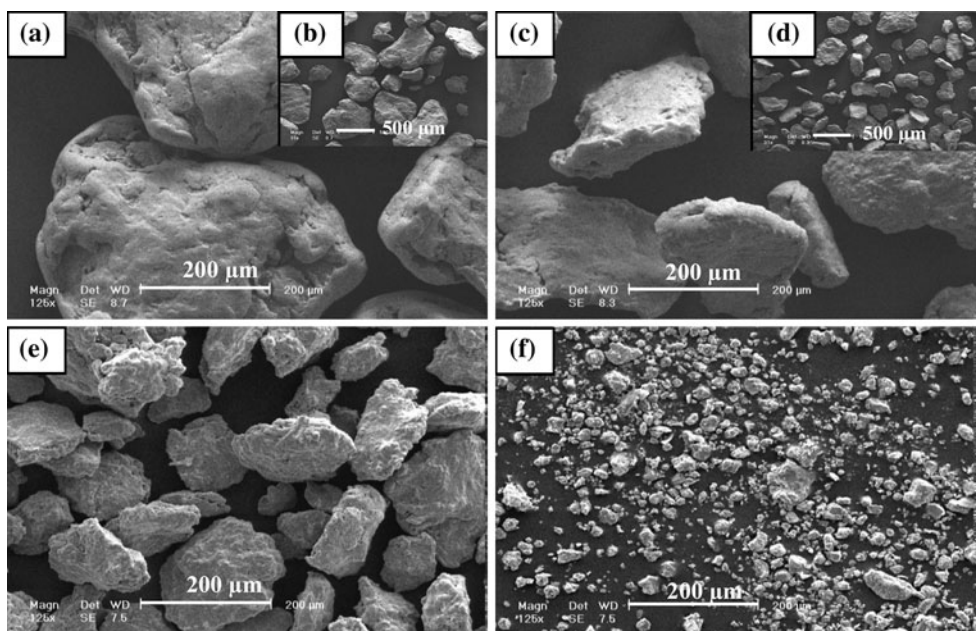
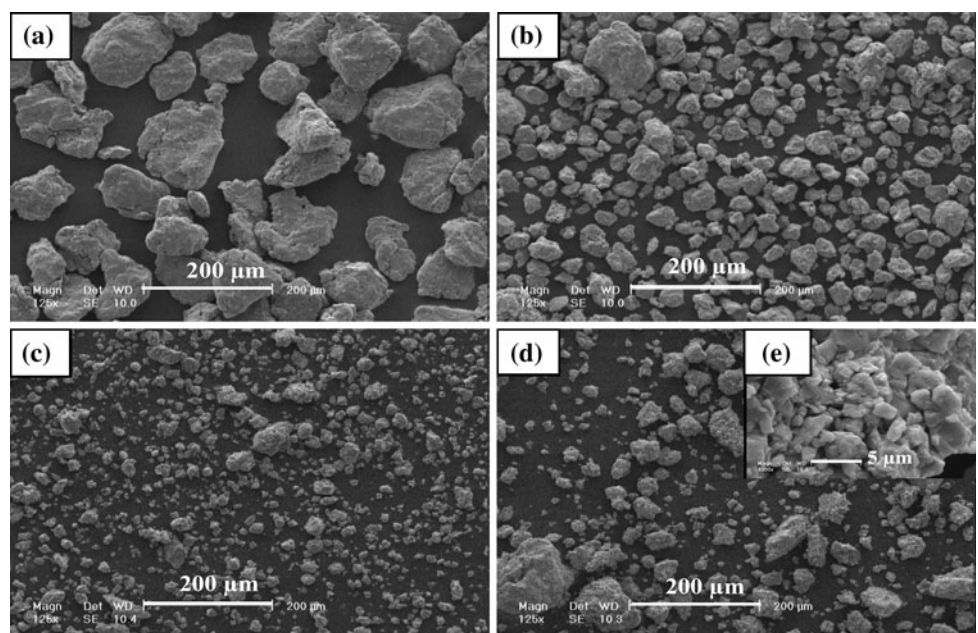
Table 1 Crystallite size and internal strain of Fe_3Al and $(\text{Fe},\text{Ti})_3\text{Al}$ phases at different conditions

Composition	Crystallite size (nm)		Internal strain (%)	
	100 h MA	100 h MA + annealing	100 h MA	100 h MA + annealing
Fe_3Al	35	35	1.76	0.93
$(\text{Fe},\text{Ti})_3\text{Al}$	12	15	1.5	0.86

increasing milling time. Also the size distribution of powder particles was nonuniform at early stages of milling but gradually became uniform with increasing milling time

up to 100 h. After 5 and 20 h of milling times the powders had flake-like morphology with mean powder particle size of about $500 \pm 200 \mu\text{m}$ and $380 \pm 110 \mu\text{m}$, respectively. This value decreased to $140 \pm 35 \mu\text{m}$ and $35 \pm 13 \mu\text{m}$ after 60 h and 100 h of milling times, respectively.

Similar to $\text{Fe}_{75}\text{Al}_{25}$ system, the mean powder particle size of $\text{Fe}_{50}\text{Al}_{25}\text{Ti}_{25}$ powder mixture (Fig. 8) decreased with increasing milling time up to 60 h. Further milling had no significant effect on powder particle size. For $\text{Fe}_{50}\text{Al}_{25}\text{Ti}_{25}$ system the mean powder particle size was about $130 \pm 15 \mu\text{m}$ after 5 h, $45 \pm 15 \mu\text{m}$ after 20 h, and $30 \pm 8 \mu\text{m}$ after 100 h of milling time.

Fig. 7 SEM images of $\text{Fe}_{75}\text{Al}_{25}$ powder particles after **a**, **b** 5 h, **c**, **d** 20 h, **e** 60 h, and **f** 100 h of milling times**Fig. 8** SEM images of $\text{Fe}_{50}\text{Al}_{25}\text{Ti}_{25}$ powder particles after **a** 5 h, **b** 20 h, **c** 60 h and **d**, **e** 100 h of milling times [11]

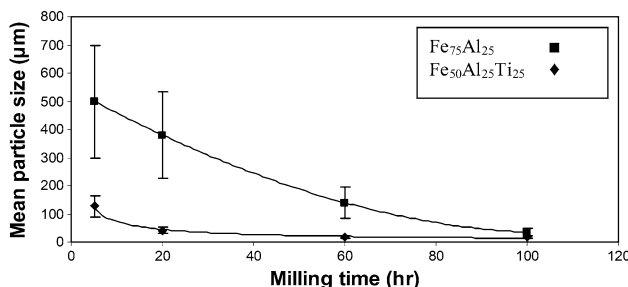


Fig. 9 Variation of mean powder particle size with milling time

Figure 9 plots the mean powder particle size of Fe₇₅Al₂₅ and Fe₅₀Al₂₅Ti₂₅ systems after different milling times. The particle size of Fe₇₅Al₂₅ powder mixture was decreased with increasing milling time. Sudden drop of the particle size was seen between 60 and 100 h of MA as a result of Fe(Al)-Fe₃Al transformation in this stage. As seen in all stages of milling times the mean powder particle size for Fe₅₀Al₂₅Ti₂₅ system is smaller than Fe₇₅Al₂₅ system. This is as a result of Ti substitution for Fe in Fe-Al system. For Fe₅₀Al₂₅Ti₂₅ system unlike Fe₇₅Al₂₅ system a Fe(Al,Ti) solid solution is formed at early stages of milling. Formation of this phase enhances the work hardening and therefore the fracturing of powder particles.

Figure 10 shows microhardness values of Fe₇₅Al₂₅ and Fe₅₀Al₂₅Ti₂₅ powder mixtures at different milling times. As seen for both compositions, microhardness value increased with increasing milling time up to 100 h. In Fe₇₅Al₂₅ powder mixture the microhardness value increased with increasing milling time up to 60 h due to the several effects including work hardening, grain refinement, and solid solution formation. After 60 h of milling time the microhardness value increased mainly as a result of formation of Fe₃Al intermetallic compound according to the XRD results.

Fe₅₀Al₂₅Ti₂₅ composition exhibited a higher hardness value compared with Fe₇₅Al₂₅ composition after the same milling times. This can be caused by the presence of Ti in Fe-Al system that increases the rate of work hardening.

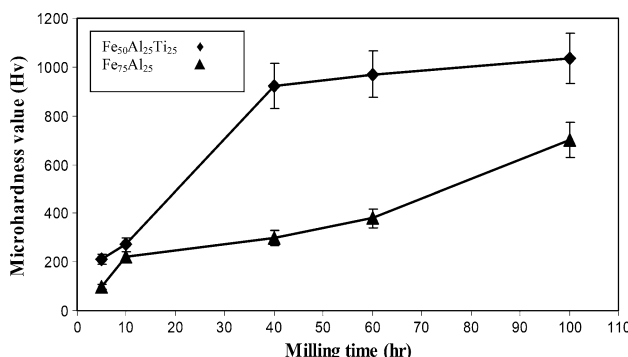


Fig. 10 Microhardness value of Fe₇₅Al₂₅ and Fe₅₀Al₂₅Ti₂₅ powder mixtures versus milling time

Zhu et al. [6] also reported that Ti-added Fe₃Al alloys exhibited significant strain hardening compared with Fe₃Al compounds. The nanocrystalline (Fe,Ti)₃Al compound exhibited the hardness value of 1050 Hv after 100 h of milling time that is significantly higher than 700 Hv obtained for nanocrystalline Fe₃Al compound.

Conclusion

Mechanical alloying of Fe-Al-Ti ternary system was performed to study the effect of Ti addition on alloying and formation of nanocrystalline structure in Fe-Al system. It was found that:

1. In both Fe₇₅Al₂₅ and Fe₅₀Al₂₅Ti₂₅ systems MA led to the formation of Fe-based solid solution which transformed to the corresponding intermetallic compounds after longer milling times.
2. The presence of Ti in Fe-Al system decreases the milling time for solid solution and intermetallic compound formation.
3. Ti substitution for Fe in Fe₃Al phase enhances the ordering of DO₃ structure upon annealing.
4. (Fe,Ti)₃Al intermetallic compound achieved a smaller crystallite size compared with Fe₃Al phase.
5. The mean powder particle size in Fe-Al-Ti system was smaller than that for Fe-Al system at all stages of milling.
6. The Fe₃Al intermetallic compound exhibited a hardness value of 700 Hv which is significantly smaller than 1050 Hv obtained for (Fe,Ti)₃Al intermetallic compound.

References

1. Gertsman VY, Dremailova O (2006) J Mater Sci 41:4490. doi: [10.1007/s10853-006-0082-z](https://doi.org/10.1007/s10853-006-0082-z)
2. Park BG, Ko SH, Park YH, Lee JH (2006) Intermetallics 14:660
3. Enayati MH, Karimzadeh F, Anvari SZ (2008) J Mater Process Technol 200:312
4. Tang HG, Ma XF, Zhao W, Yan XW, Hong RJ (2002) J Alloys Compd 347:228
5. Morris DG, Dadras M, Morris MA (1993) J Phys III 3:429
6. Zhu SM, Sakamoto K, Tamura M, Iwasaki K (2001) Mater Trans 42:484
7. Chungcheng H, Zuolin C, Yansheng Y, Zhikan Z (2002) J Nanoparticle Res 4:107
8. Suryanarayana C (2001) Prog Mater Sci 46:1
9. Maupin HE, Wilson RD, Hawk JA (1993) Wear 162–164:432
10. Zhu SM, Iwasaki K (1999) Mater Sci Eng A270:170
11. Rafiei M, Enayati MH, Karimzadeh F (2009) J Alloys Compd 480:392
12. Enayati MH, Salehi M (2005) J Mater Sci 40:3933. doi: [10.1007/s10853-005-0718-4](https://doi.org/10.1007/s10853-005-0718-4)
13. Williamson GK, Hall WH (1953) Acta Metal 1:22